

## **ELECTRO-ACOUSTIC INFLUENCE OF THE MEASURING SYSTEM ON THE PHOTOACOUSTIC SIGNAL AMPLITUDE AND PHASE IN FREQUENCY DOMAIN<sup>†</sup>**

*UDC 534.63:681.11.031.24:534.83*

**Sanja M. Aleksić<sup>1\*</sup>, D. K. Markushev<sup>1</sup>, Dragan S. Pantić<sup>1</sup>,  
Mihajlo D. Rabasović<sup>2</sup>, Dragan D. Markushev<sup>2</sup>, Dragan M. Todorović<sup>3</sup>**

<sup>1</sup>Faculty of Electronic Engineering, University of Niš, Niš, Serbia

<sup>2</sup>Institute of Physics, University of Belgrade, Belgrade-Zemun, Serbia

<sup>3</sup>Institute for Multidisciplinary Research, University of Belgrade, Belgrade, Serbia

**Abstract.** *The paper discusses the most common impacts of the measuring system on the amplitude and phase of the photoacoustic signals in the frequency domain using the open-cell experimental set-up. The highest signal distortions are detected at the ends of the observed modulation frequency range from 20 Hz to 20 kHz. The attenuation of the signal is observed at lower frequencies, caused by the electronic filtering of the microphone and sound card, with characteristic frequencies of 15 Hz and 25 Hz. At higher frequencies, the dominant signal distortions are caused by the microphone acoustic filtering, having characteristic frequencies around 9 kHz and 15 kHz. It has been found that the microphone incoherent noise, the so called flicker noise, is negligibly small in comparison to the signal and does not affect the signal shape. However, a coherent noise originating from the power modulation system of the light source significantly affects the shape of the signal in the range greater than 10 kHz. The effects of the coherent noise and measuring system influence are eliminated completely using the relevant signal correction procedure targeting the photoacoustic signal generated by the sample.*

**Key words:** *electro-acoustic, photoacoustic signal, measuring system, amplitude, phase, frequency domain*

### 1. INTRODUCTION

The detection of the acoustic signal coming from a sample illuminated by the modulated radiation (Marquerinit et al., 1991; Perondi and Miranda, 1987; Vargas and Miranda, 1988)

---

Received January 09<sup>th</sup>, 2015; accepted Jun 2<sup>nd</sup>, 2016

<sup>†</sup> **Acknowledgement:** This research was supported by the Ministry of Education, Science and Technological Development of the Republic of Serbia (projects ON171016)..

\* **Corresponding author:** Sanja Aleksić

Faculty of Electronic Engineering, University of Niš, Aleksandra Medvedeva 14, 18000 Niš, Serbia

E-mail: sanja.aleksic@elfak.ni.ac.rs

represents the basis of all open-cell photoacoustic (PA) measurements. The signal amplitude and phase changes are monitored in the modulation frequency domain of 20 Hz to 20 kHz (Rabasović *et al.*, 2009; Todorović *et al.*, 2014).

Ideally, the measured PA signal corresponds to the signal from the sample in the entire frequency domain. However, in reality this is not true. First, there is a big influence of noise that comes from different sources. Second, there is some influence of the instruments applied within the experimental system that distorts the signal, especially at the ends of the frequency interval (Markushev *et al.*, 2015; Todorović *et al.*, 2013).

In the open-cell photoacoustic spectroscopy, the microphone with associated electronics and the lock-in amplifier (Marquerinit *et al.*, 1991; Somer *et al.*, 2013) play the major role in the experiments. A microphone is an acoustic-to-electric transducer that converts sound into an electrical signal. Because of differences in their construction, microphones respond differently to a sound. This difference in response produces a non-uniform phase and frequency responses, usually recognized as filtering. Electret microphones are the most commonly used microphones in photoacoustics, having a wide frequency response from 10 Hz to 30 kHz (Albert *et al.*, 1993). At low frequencies ( $< 1$  kHz), these microphones usually act as electronic high-pass filters attenuating the signal amplitude increasing the phase simultaneously. At higher frequencies ( $> 1$  kHz), an electret microphone usually behaves as an acoustic low-pass filter changing the amplitude and decreasing the phase simultaneously. A lock-in amplifier is a type of amplifier that can extract a signal amplitude and phase from an extremely noisy environment (Scofield, 1994; Burdett, 2005), even though there are many types of noises and deviations due to the influence of the used instruments that no lock-in can remove. A good replacement for a lock-in could be the computer sound card. The computer sound card has proven as reliable as the lock-in for the given frequency domain. A special attention should be paid to the fact that each sound card has its own electrical characteristics which may be expressed in terms of the electronic high-pass filters with typical  $RC$  values and characteristic frequencies below 20 Hz.

In photoacoustics, noise is a general term used for all unwanted signals observed at the output of the detection system, masking the true PA signal of interest (Telenkov and Mandelis, 2010; Lashkari and Mandelis, 2010). Noise signals are usually random in both amplitude and phase, and carry no useful information. Coherent noise may also be present, interfering with the true PA signal as a consequence of the optical source modulation system influence. Both kinds of noise can be classified by their statistical properties of the modulation frequency  $f$  power-low dependence and by how they modify the true PA signal (additive, multiplicative, etc).

This paper analyses the most common causes of the PA signal distortion in the frequency domain, caused by the used detector, instruments and supporting electronics in the described experiments. The signal correction procedure is presented on the measured acoustic signals collected by the microphone, using illuminated 100  $\mu\text{m}$  thick Si plates as a PA signal generator. Independent measurements of noise are performed with the purpose of recognizing the flicker and coherent signal deviations as the dominant ones. Besides the noise subtraction, the paper also explores the way in which the signal fitting procedure can be applied to obtain and remove instrumental influences recognized as electronic high-pass and acoustic low-pass filtering, targeting the PA signal of interest.

## 2. ELECTRONIC HIGH-PASS FILTERS

A high-pass filter is an electronic filter that passes signals with a frequency higher than a certain cut-off frequency and attenuates signals with frequencies lower than a cut-off frequency. Knowing the construction and inner parts characteristics, it is well known that electret microphones can be considered to be high-pass filters, as well. A cross section of the entire electret microphone module used in our experiments and its equivalent electrical schematic are shown in Fig. 1 (Albert et al., 1993).

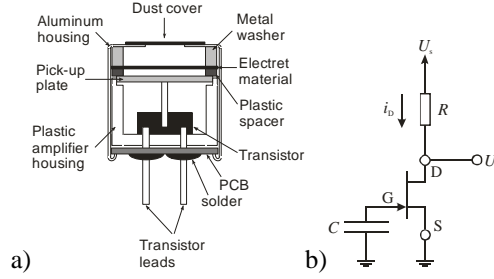


**Fig. 1** a) A cross section and b) equivalent schematic the electret microphone used for open-cell photoacoustic measurements.  $R$  is the resistance,  $C$  is the capacitance, G, S and D are the transistor pins called gate, source and drain respectively,  $i_D$  is the drain current,  $U_0$  and  $U_s$  are the relevant voltages.

A transistor is used as the amplifier in this case because it has a really high input resistance (sometimes in Mohms range). This means that almost no current is pulled off the electret capacitor. Sometimes manufacturers make the transistors with a lower input resistance, which affects the low frequency response of the microphone. This happens because the input stage acts like a high-pass filter, with the electret being the capacitor, and the input of the amplifier being the resistor, whereas larger values of  $R$  and  $C$  give lower cut-off frequencies.

A high non-linear microphone response at low frequencies and 3-D effects influence on amplitude and phase behavior are two main problems in our measurements. One must be very careful to distinguish these effects from the unadjusted microphone output impedance and inputs impedance of the electronic detection system (lock-in amplifier or sound card).

To avoid non-linear microphone response at low frequencies, we work with relatively low intensity PA signals. Thus the nonlinear effects are less problematic, because they are primarily related to the high intensity signals. On the other hand, non-homogeneous sample irradiation could enhance 3-D effect and change the signal behavior in low frequencies domain. This is the reason why we attempt to irradiate sample homogeneously in order to minimize the influence of the 3-D effect.

All the experiments performed using an electret microphone as a signal transducer emphasize that this kind of microphone can be regarded as the simple first-order electronic high-pass filter. The product of the resistance  $R$  and capacitance  $C$  ( $R \times C$ ) is the time constant ( $\tau_c$ ); it is inversely proportional to the cut-off frequency  $f_c$ . The transfer function  $H^e(j\omega)$  for this kind of filter has the form:

$$H^e(j\omega) = \frac{\omega\tau_c}{(1 + j\omega \cdot \tau_c)}, \quad (1)$$

where  $\omega = 2\pi f$  and  $\tau_c = (2\pi f_c)^{-1}$ . At high frequencies,  $f \gg f_c$ , the capacitor acts as a short signal and the gain is 1 (the signal is passed). At low frequencies,  $f \ll f_c$ , the capacitor is open and the output is zero (the signal is blocked).

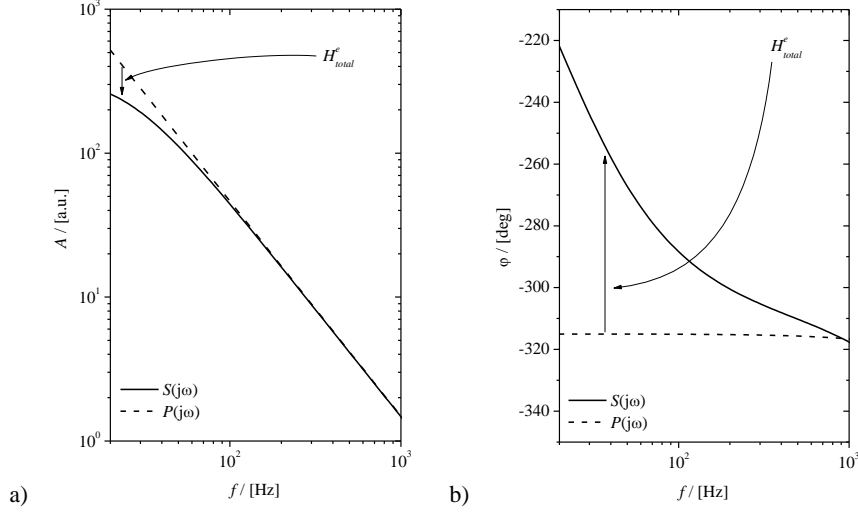


**Fig. 2** Typical high-pass filter effects on our simulated signal a) amplitude  $A$  and b) phase  $\varphi$ .  $S(j\omega)$  is the measured signal picked-up by the instruments,  $P(j\omega)$  is the signal generated by the sample and  $H_{total}^e(j\omega)$  is the measurement system influence. Arrows shows the level of  $P(j\omega)$  distortion.

The high-pass filter effects in our photoacoustic system are accounted for using a first-order high-pass filter cascade system transfer function  $H_{total}^e(j\omega)$  [6]:

$$H_{total}^e(j\omega) = H_1^e(j\omega) \cdot H_2^e(j\omega) = -\frac{\omega\tau_{c1}}{(1 + j\omega \cdot \tau_{c1})} \cdot \frac{\omega\tau_{c2}}{(1 + j\omega \cdot \tau_{c2})}, \quad (2)$$

where  $\tau_{c1} = (2\pi f_{c1})^{-1}$  and  $\tau_{c2} = (2\pi f_{c2})^{-1}$  are the time constants of the microphone and signal processing electronics, usually the sound-card or lock-in.

In general, the transfer function defined with equation (2) explains the PA signal distortion originated from the instruments used to construct the apparatus. Although we find that two high-pass filters are appropriate, there is no reason why one or even more than two would not be appropriate for other apparatuses (Markushev *et al.*, 2015). The signal  $S(j\omega)$  detected by our microphone and sound-card in the low frequency range ( $f < 1$  kHz) is the product of the photoacoustic signal generated by sample  $P(j\omega)$  and  $H_{total}^e(j\omega)$ . Typical high-pass filter effects on our simulated PA signal amplitude  $A$  and phase  $\varphi$  are presented in Fig. 2.

### 3. ACOUSTIC LOW PASS FILTERS

Because of differences in their construction (especially diaphragm material and geometry), electret microphones have their own characteristic responses to a sound (Albert *et al.*, 1993).

This difference in response produces non-uniform frequency responses at frequencies higher than 5 kHz. The reason for that lies in the fact that the microphone body can be considered in the first approximation as an acoustic resonator, allowing the air flow inside the microphone volume conducted by the diaphragm movements and microphone geometry.

If one removes the dust cover from the microphone front (Fig. 1.a), the volume between the microphone opening and diaphragm (electret material) can be considered to be the acoustic system shown in Fig. 3:

$U_v$  represents the volume velocity, and  $M_a$ ,  $C_a$  and  $R_a$  are the respective acoustic inertance, compliance and resistance components of the system. The simple open cavity system presented in Fig. 3 is very similar in form to a Helmholtz resonator, with the exception that we have introduced an exit hole instead of a diaphragm into the end wall of the cavity. We assume that the diaphragm has walls of a negligible thickness compared to its diameter. This allows us to ignore any inductance and acoustic resistance effects at the exit hole.

The electrical equivalent circuit for the presented acoustic system (Fig. 3) is depicted in Fig. 4. It can be recognized as the common second order low-pass filter circuit.

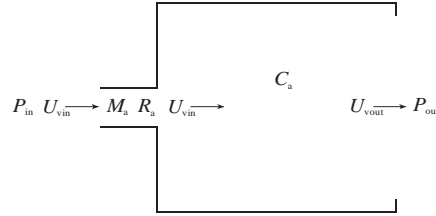


**Fig. 3** The simple open cavity system as an acoustic analogue to the electret microphone volume between the opening and diaphragm.

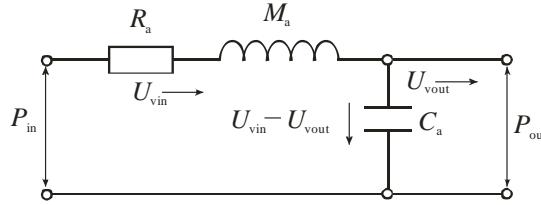


**Fig. 4** The electrical equivalent circuit for acoustic system presented in Fig. 3

The transfer function  $H^a(j\omega)$  for this circuit is quite simple:

$$H^a(j\omega) = \frac{1}{\frac{C_a M_a}{1 + \frac{R_a}{M_a} j\omega + (j\omega)^2}}, \quad (3.a)$$

or

$$H^a(j\omega) = \frac{\omega_c^2}{\omega_c^2 + j\delta_c \omega - \omega^2}, \quad (3.b)$$

where  $\omega_c = 2\pi f_c = 1/C_a M_a$  is the cut-off frequency and  $\delta_c = R_a/M_a$  is the damping factor. A complete electro-acoustic together with the mechanical equivalents are explained in details in the text ([http://www.moultonworld.pwp.blueyonder.co.uk/Lecture9\\_page.htm](http://www.moultonworld.pwp.blueyonder.co.uk/Lecture9_page.htm)).

The main source of the signal distortion in our measurements is the microphone diaphragm behavior in the frequency domain. It means that the air flow changes within the microphone volume are mainly conducted by diaphragm movements. How it moves depends,

among other things, on the material that diaphragm is made of. Electret microphones typically use Mylar plastic as the diaphragm material. The exact formula of Mylar used is a trade secret and is probably different for each microphone company. Moreover, diaphragms are usually light and flexible, so they can bend in a number of ways, producing an uneven frequency response with a typical cut-off frequency which depends on a manufacturer.

Usually, diaphragm movement effects are accompanied by the effects of the microphone geometry. A smaller microphone body means a stronger signal and possible resonant effects at higher frequencies. A smaller diaphragm diameter means less signal distortion. Combined, these "smaller" characteristics could produce an acoustic response in the frequency domain characterized also by a typical cut-off frequency.

Based on our experimental results, taking into account all mentioned geometric and material type effects in the terms of acoustic filtering, a general expression of the microphone response described as acoustic low-pass filters may be shown, represented by a combination of second-order low-pass filters:

$$H_{total}^a(j\omega) = \frac{\omega_{c3}^2}{\omega_{c3}^2 + j\delta_{c3}\omega - \omega^2} + \frac{\omega_{c4}^2}{\omega_{c4}^2 + j\delta_{c4}\omega - \omega^2}, \quad (4)$$

where  $\delta_k$  is the damping factor ( $k = c3, c4$ ),  $\omega_{c3}$  is the microphone cut-off frequency and  $\omega_{c4}$  is the characteristic frequency which depends on the geometry of the microphone body. The kind of filters combination used depends on experimental conditions and instruments. Our previous study described the cascade system and its influence. But our experimental results (especially phase measurements) obtained by the use of different materials and under different conditions prove that the best combination of acoustic filters is presented by equation (4). A typical frequency response of our measurement system explained by the influence of acoustic low-pass filters is depicted in Fig. 5.

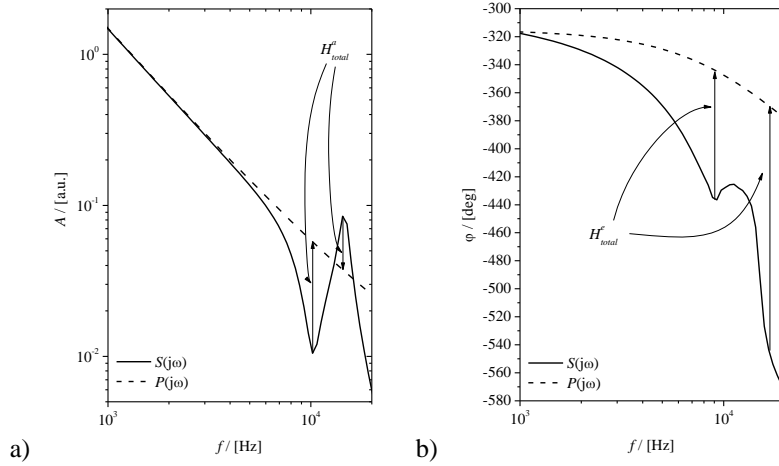


**Fig. 5** Typical acoustic low-pass filter effects on our simulated signal a) amplitude  $A$  and b) phase  $\varphi$ .  $S(j\omega)$  is the measured signal picked-up by the instruments,  $P(j\omega)$  is the signal generated by the sample and  $H_{total}^e(j\omega)$  is the measurement system influence. Arrows shows the level of  $P(j\omega)$  distortion.

## 4. NOISE

Several sources of noise are found in photoacoustic measurements using an open-cell. These include: a) random Brownian noise, b) flicker noise and c) coherent crosstalk noise. All represent additive types of noise and add to the underlying PA signal. Brownian or the random walk noise, is proportional to  $f^{-2}$ . The electronic flicker noise has a  $f^{-1}$  dependence. The coherent crosstalk noise is a power-low noise directly proportional to  $f^{+1}$ . The frequency dependent noise amplitude measurements for our open photoacoustic cell are presented in Fig. 6. These results show that Brownian ( $f^{-2.0}$ ), flicker ( $f^{-1.0}$ ) and crosstalk ( $f^{+1.0}$ ) noise can be recognized in a wide modulation frequency range. In the case of 20 Hz – 20 kHz domain, the flicker and crosstalk noise are dominant. This is the reason why the total noise  $N(j\omega)$  in photoacoustic measurements may be presented in this form:

$$N(j\omega) = N_{FN}(j\omega) + N_{CSD}(j\omega), \quad (5)$$

where  $N_{FN}(j\omega)$  is the flicker noise, and  $N_{CSD}(j\omega)$  is the crosstalk or coherent signal deviation (CSD). The flicker noise cannot be reduced but the coherent signal deviation can be subtracted. Usually, the flicker noise has a negligible influence on the PA signal amplitude ( $f^{-1.5}$ ) in the mentioned frequency range.

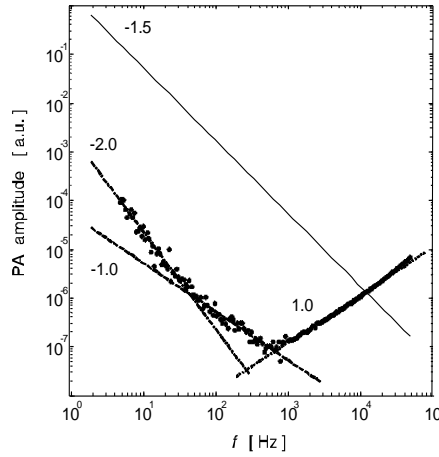


**Fig. 6** Theoretically obtained PA signal with  $f^{1.5}$  slope (full line), together with noise measurements (circles): Brownian ( $f^{2.0}$ , dash-dotted line), flicker ( $f^{1.0}$ , dashed line) and crosstalk ( $f^{1.0}$ , dotted line) noise.

Here, the PA signal is calculated theoretically in the case of Si thin plates and assuming thermal diffusion as a dominant process. The crosstalk noise is found to be coupled with the PA signal at higher frequencies ( $>10$  kHz). Based on the results, a noise reduction is needed to remove the crosstalk signal from the measurements. One must bear in mind that the noise reduction will give the signal clear from noise but not from system deviations.

## 5. EXPERIMENT, RESULTS AND DISCUSSION

All our experiments are based on the transmission open-cell photoacoustic set-up. It assumes that the investigated sample in the form of a circular or rectangular plate is placed instead of a dust cover (Fig. 1). A Rubber o-ring is placed between the sample and aluminum housing to prevent a direct contact with the microphone body and to define mechanical conditions to allow the sample bending. The volume between the sample and diaphragm (electret material) is considered as the photoacoustic cell, having the form presented in Figure 3. The sample is periodically heated by a photo-thermal effect with a modulated light source (various LEDs or laser diodes). A periodic sample heating followed by an expansion and bending causes periodic pressure waves which are detected by the microphone and registered by the lock-in or sound card as a measurement result in the terms of the amplitude and phase.

The measurement result  $Y(j\omega)$  can be expressed by the sum of the signal  $S(j\omega)$  and noise  $N(j\omega)$  components:

$$Y(j\omega) = S(j\omega) + N(j\omega). \quad (6)$$

The  $N(j\omega)$  is defined by equation (5) and the signal  $S(j\omega)$ , the so called distorted signal, is defined by

$$S(j\omega) = P(j\omega)H(j\omega), \quad (7)$$

where  $H(j\omega) = H_{total}^e(j\omega)H_{total}^a(j\omega)$  is the measurement system electro-acoustic response defined by equations 2 and 4. The  $P(j\omega)$  represents the photoacoustic signal generated by the sample, the so called the “true” PA signal.

The main goal of our experiment is to reach the  $P(j\omega)$  and extract the thermal and mechanical parameters of the sample. It can be done applying the signal correction process given in the following steps: 1) Find the experimental conditions to allow the highest signal to noise ratio and neglect the flicker noise  $N_{FN}(j\omega)$ ; 2) Measure and subtract the coherent signal deviations  $N_{CSD}(j\omega)$  from the  $Y(j\omega)$  to obtain  $S(j\omega)$  using equation (6); 3) Fit  $S(j\omega)$  to obtain all microphone and lock-in electro-acoustic characteristics using equations 2 and 4; 4) Correct  $S(j\omega)$  by removing all detected deviations in  $H(\omega)$ , targeting the “true” PA signal  $P(j\omega)$ .

**Table 1** Si sample bulk parameters

Density	$\rho = 2.33 \cdot 10^3 \text{ kgm}^{-3}$	Coefficient of carrier diffusion	$D_n = 1.2 \cdot 10^{-3}$
Optical reflectivity	$R = 0.30$	Recombination velocity of the front surface	$s_1 = 2 \text{ ms}^{-1}$
Optical absorption coefficient	$\beta = 5.00 \cdot 10^5 \text{ m}^{-1}$	Recombination velocity of the rear surface	$s_2 = 24 \text{ ms}^{-1}$
Thermal diffusivity	$D_s = 1.00 \cdot 10^{-4} \text{ m}^2 \text{ s}^{-1}$	Young's modulus	$E = 1.31 \cdot 10^{11} \text{ Nm}^2$
Excitation energy	$\varepsilon = 1.88 \text{ eV}$	Linear Thermal expansion	$\alpha = 3.0 \cdot 10^{-6} \text{ K}^{-1}$
Energy gap	$\varepsilon_g = 1.11 \text{ eV}$	Coefficient of electronic deformation	$d_n = -9.0 \cdot 10^{-31} \text{ m}^3$
Lifetime of photogenerated carriers	$\tau = 6.0 \cdot 10^{-6} \text{ s}$		

For this kind of analysis, we performed the test using a thin Si plate sample, prepared from 3 – 5  $\Omega\text{cm}$ , n-type, <100> oriented Si wafer, with the constant bulk values given in Table 1 as a PA signal generator. Because the Si plate is well-characterized (Markushev et al., 2015), we used it as a calibration sample to deduce the apparatus constants.

Si is a very convenient material as a test sample. The developed technological processes in microelectronic and optoelectronic integrated devices production enable to obtain Si wafers with perfect crystalline structures and electronic purity. Commercial Si wafers, due to their wide application, with advance well-known physical characteristics, are perhaps the most suitable as test samples. On the other hand, Si has perfect elastic characteristics and it is an ideal material in production of micromechanical structures by applying the integrated devices production technological processes. The standard microelectronic technologies enable the production of thin elastic structures (for example with a thickness of much less than 100  $\mu\text{m}$  with diameter 10 mm), with good repeatability characteristics. For example, practically it is not possible to make a thin plate with graphite (these plates are very brittle and cannot be fixed on the microphone).

It should be noted that in the measurement methods applied in this study, the sample is mounted on a microphone so as to ensure good sealing of microphone measuring chamber. In addition, only fixing the sample must be well defined to ensure repeatable elastic vibration characteristics of the sample. In this regard, the Si wafer is shown as the most suitable. After all, MEMS technology is based on silicon as a basic material.

Fig. 7 depicts the measured signal  $Y(j\omega)$  of the 100  $\mu\text{m}$  thick Si plate in a) amplitude,  $A(f)$ , and b) phase,  $\varphi(f)$ , (solid line + asterisks) as a function of the modulation frequency  $f$ . The noise amplitude and phase (line + circles) are measured using the blank beam block. The measured flicker noise,  $N_{\text{FN}}(\omega)$ , having the  $f^{-1.0}$  amplitude dependence, is dominant but negligible (signal-to-noise ratio greater than  $10^3$ ). The  $N_{\text{CSD}}(\omega)$  amplitude, having the  $f^{+1.0}$  dependence, is very high and intercepts the PA signal within the (10 – 20) kHz range. One must bear in mind that the CSD interference must be measured carefully and removed from the measurement result  $Y(j\omega)$  (equation (6)). After the subtractive  $N_{\text{CSD}}(\omega)$  removal, the “clear” signal  $S(j\omega)$  amplitude and phase are shown (dashed line) in comparison to the nascent data. The “clear” signal accounts for CSD, but not instrumental distortion.

Using our experimental set-up with blank beam block and microphone turned off we are able to observe some electrical line interference at 50 Hz. But, our microphone is battery-powered and the influence of electrical line interference is significantly reduced. Careful noise analysis in our experiments shows that such kind of interference has a negligible influence on the measured signal.

Following the  $S(j\omega)$  fitting procedure and equation (7), one can determine the electro-acoustic system characteristics in the low-frequency range using equation 1 to 4 (see Fig. 8). As expected, the  $H^e_{\text{total}}(j\omega)$  deviation decreases the signal amplitude. The fitting yields the respective sound card and detector characteristic modulation frequencies,  $f_{\text{eLF1}} = (15 \pm 3)\text{Hz}$  and  $f_{\text{eLF2}} = (25 \pm 1)\text{Hz}$ .

Using Eq.(4), the characteristic detector acoustic parameters are found to be:  $f_{\text{c3}} = (9.4 \pm 0.3) \cdot 10^3\text{Hz}$ ,  $\delta_{\text{c3}} = (0.45 \pm 0.05) \cdot \omega_{\text{c4}}$ ,  $f_{\text{c4}} = (14.7 \pm 0.5) \cdot 10^3\text{Hz}$  and  $\delta_{\text{c4}} = (0.08 \pm 0.01) \cdot \omega_{\text{c3}}$ . The  $f_{\text{c4}}$  approximates the microphone cut-off frequency. The solid arrows in Fig. 8.a and b show that the influence  $H(j\omega) = H^e_{\text{total}}(j\omega) H^a_{\text{total}}(j\omega)$  on  $P(j\omega)$ . It is a reasonable assumption that the corrected signals  $P(j\omega)$  match the theoretical ones, obtained using the standard

photoacoustic theoretical models (Rosencwaig and Gersho, 1976; Roussel, 1983; McDonald and Westel, 1978).

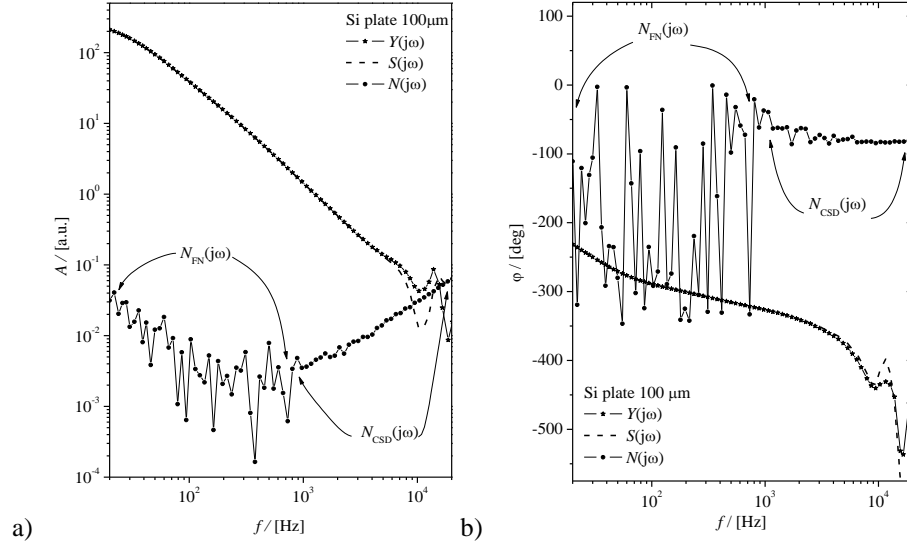


**Fig. 7** Typical 100  $\mu\text{m}$  thick Si plate measured photoacoustic signal  $Y(j\omega)$  a) amplitude  $A$  and b) phase  $\phi$ .  $S(j\omega)$  is the signal “clear” from CSD and  $N(j\omega)$  is the noise.

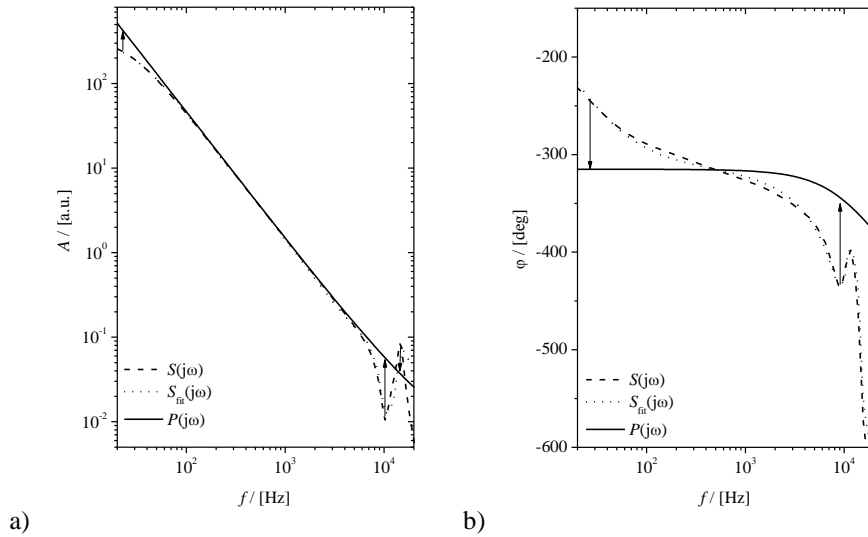


**Fig. 8** Typical measured signal  $S(j\omega)$  a) amplitude  $A$  and b) phase  $\phi$  picked-up by the instruments.  $P(j\omega)$  is the signal generated by the sample and  $S_{\text{fit}}(j\omega)$  is the fitting curve. Arrows shows the level of  $P(j\omega)$  correction.

## 6. CONCLUSIONS

Our open-cell photoacoustic measurements of a 100 $\mu\text{m}$  Si plate over a 20 Hz to 20 kHz modulation frequency range show that the measured PA signals can be represented as a combination of a signal distorted by the electro-acoustic filtering and noise. It was shown that an accurate photoacoustic signal generated by the sample can be obtained using noise and signal deviation recognition and removal procedures based on the recognition of electro-acoustic processes giving rise to a signal distortion. We find the flicker noise to be negligible in the whole frequency range and the coherent noise to be the dominant interference at high frequencies. Its origin was found to be the current optical excitation source modulation system.

It was found that the coherent noise subtraction procedure is sufficient to obtain an interference-free signal. A further analysis reveals strong signal distortions at the end of the frequency domain. At low frequencies, an apparent amplitude and phase distortion was found for  $f < 1000$  Hz. This distortion was attributed to the electronic high-pass filtering of the microphone and the sound card used instead of the lock-in. The interference-free signal correction procedure allows one to estimate the instrument characteristic frequency for the detector (25 Hz) and the sound-card (15 Hz).

Major system signal distortions were detected in the high frequency range ( $f > 1000$  Hz) and attributed mainly to the acoustic detector characteristics. In the open-cell configuration, the electret microphone acts as an acoustic low-pass filter. Two characteristic frequencies were found. The first was the microphone cut-off frequency (14.9 kHz) attributed to the diaphragm properties. The second was attributed to the microphone geometry.

A proper signal correction procedure yields to the corrected signal that appears to be an accurate representation of the theoretical PA amplitude and phase signal for the 100  $\mu\text{m}$  thick Si plate. It was found out that this procedure should be valid for all solid samples and is suitable for multilayered samples composed of a substrate and a thin film as a coating, as long as the frequency-dependent PA effects are accounted for.

## REFERENCES

- Albert A., van der Woerdan Wouter C., Serdijn A., 1993. Low-voltage low-power controllable preamplifier for electret microphones", IEEE Journal of Solid-State Circuits, vol. 28, 10.
- Burdett R., 2005, Amplitude modulated signals - the lock-in amplifier, Handbook of Measuring System Design, Wiley, New York, ISBN. 978-0-470-02143-9.
- [http://www.moultonworld.pwp.blueyonder.co.uk/Lecture9\\_page.htm](http://www.moultonworld.pwp.blueyonder.co.uk/Lecture9_page.htm)
- Lashkari B., Mandelis A., 2011. Comparison between pulsed laser and frequency-domain photoacoustic modalities: Signal-to-noise ratio, contrast, resolution, and maximum depth detectivity, Review of Scientific Instruments, vol. 82, 094903.
- Markushev D. D., Rabasović M.D, Todorović D.M., Galović S., Bialkowski S. E., 2015. Photoacoustic signal and noise analysis for Si thin plate: Signal correction in frequency domain, Review of Scientific Instruments vol. 86, 035110; doi: 10.1063/1.4914894.
- Marquerinit M.V, Cellat N., Mansanares A.M., Vargas H., Miranda L.C.M., 1991. Open photoacoustic cell spectroscopy, Measurement, Science & Technology, vol. 2, pp. 396-401.
- Marquerinit MV, Cellat N, Mansanarest A.M, Vargas H, Miranda L.C.M., 1991. Open photoacoustic cell spectroscopy, Measurement, Science & Technology, vol. 2, pp. 396-401.
- McDonald F., Westel G. 1978. Generalized theory of the photoacoustic effect, Journal of Applied Physics, vol. 49, pp. 2313-2322.
- Perondi L.F., Miranda L.C.M., 1987. Minimal-volume photoacoustic cell measurement of thermal diffusivity: Effect of thermoelastic sample bending, Journal of Applied Physics, vol. 62, pp. 2955-2959.

- Rabasović M.D., Nikolić M.G., Dramićanin M.D., Franko M., Markushev, 2009. Low-cost, portable photoacoustic setup for solid samples, *Measurement, Science & Technology*, vol. 20, 095902 (6pp), doi:10.1088/0957-0233/20/9/095902.
- Rosencwaig A, Gersho A., 1976. Theory of the photoacoustic effect with solids, *Journal of Applied Physics*, vol. 47, pp. 64-69.
- Roussel G., Lepoutre F., Bertrand L., 1983. Influence of thermoelastic bending on photoacoustic experiments related to measurements of thermal diffusivity of metals, *Journal of Applied Physics*, vol. 54, pp. 2383-2391.
- Scofield J.H., 1994. Frequency-domain description of a lock-in amplifier, *American Journal of Physics (AAPT)*, vol. 62, pp. 129-133.
- Somer A., Camilotti F., Costa G.F., Bonardi C., Novatski A., Andrade A.V.C., Kozłowski V.A., Jr., Cruz G.K., 2013. The thermoelastic bending and thermal diffusion processes influence on photoacoustic signal generation using open photoacoustic cell technique, *Journal of Applied Physics*, vol. 114, 063503.
- Telenkov S., Mandelis A., 2010. Signal-to-noise analysis of biomedical photoacoustic measurements in time and frequency domains, *Review of Scientific Instruments*, vol. 81, 124901.
- Todorović D.M., Markushev D., Rabasović M.D., 2013. Photoacoustic elastic bending in thin film - Substrate system, *Journal of Applied Physics*, vol. 114, 213510; doi: 10.1063/1.4839835.
- Todorović D.M., Rabasović M.D., Markushev D. D., Sarajlić M., 2014. Photoacoustic elastic bending in thin film-substrate system: Experimental determination of the thin film parameters, *Journal of Applied Physics*, vol. 116, 053506.
- Vargas H., Miranda L.C.M., 1988. Photoacoustic and Related Photothermal Techniques, *Phys. Rep.*, vol. 16, pp. 45-101.

## **ELEKTRO-AKUSTIČKI UTICAJ MERNOG SISTEMA NA AMPLITUDU I FAZU FOTOAKUSTIČKOG SIGNALA U FREKVENTNOM DOMENU**

*U ovom radu je prikazan najčešći uticaj mernog sistema na amplitudu i fazu fotoakustičkog signala u frekventnom domenu, korišćenjem eksperimentalne postavke otvorene ćelije. Najveće izobličenje signala uočeno je na krajevima posmatrane oblasti frekvencija modulacije od 20 Hz do 20 kHz. Na niskim frekvencijama primećeno je slabljenje signala prouzrokovano ponašanjem mikrofona i zvučne kartice kao elektronskih filtera, sa karakterističnim frekvencijama od 15 Hz and 25 Hz. Na višim frekvencijama dominantno izobličenje signala prouzrokovano je od strane mikrofona koji se ponaša i kao akustički filter, sa karakterističnim frekvencijama oko 9 kHz i 15 kHz. Pronađeno je da je mikrofonski nekoherentni šum, tzv. flickeršum, zanemarljivo mali u odnosu na signal, tako da ne utiče na njegov oblik. Ali, uočeno je da koherentni šum, koji potiče od sistema za modulaciju svetlosnog izvora, jako utiče na oblik signala u oblastima iznad 10 kHz. Efekti koherentnog šuma i mernog sistema mogu se eliminisati korišćenjem relevantne procedure korekcije signala težeći ka fotoakustičkom signalu koji potiče samo od uzoraka.*

Ključne reči: *elektro-akustika, foto-akustični signal, merni sistem, amplituda, faza, frekventni domen.*